Korean Journal of Radiology

KJR

# Common Postmortem Computed Tomography Findings Following Atraumatic Death: Differentiation between Normal Postmortem Changes and Pathologic Lesions

Masanori Ishida, MD, PhD[1, 2], Wataru Gonoi, MD, PhD[1], Hidemi Okuma, MD[1], Go Shirota, MD[1], Yukako Shintani, MD, PhD[3], Hiroyuki Abe, MD, PhD[3], Yutaka Takazawa, MD, PhD[3], Masashi Fukayama, MD, PhD[3], Kuni Ohtomo, MD, PhD[1]

Departments of [1]Radiology and [3]Pathology, Graduate School of Medicine, The University of Tokyo, Tokyo 113-8655, Japan; [2]Department of Radiology, Mutual Aid Association for Tokyo Metropolitan Teachers and Officials, Sanraku Hospital, Tokyo 101-8326, Japan

Computed tomography (CT) is widely used in postmortem investigations as an adjunct to the traditional autopsy in forensic medicine. To date, several studies have described postmortem CT findings as being caused by normal postmortem changes. However, on interpretation, postmortem CT findings that are seemingly due to normal postmortem changes initially, may not have been mere postmortem artifacts. In this pictorial essay, we describe the common postmortem CT findings in cases of atraumatic in-hospital death and describe the diagnostic pitfalls of normal postmortem changes that can mimic real pathologic lesions.
**Index terms:** *Autopsy imaging; Forensic radiology; Postmortem CT; Postmortem imaging*

## INTRODUCTION

Postmortem computed tomography (CT) has increased in importance as an adjunct to traditional autopsy in forensic medicine (1-4). Diagnostic guidelines for postmortem imaging are being established worldwide, and postmortem CT findings in several organs have been described (5-

10). Normal postmortem changes should be recognized when interpreting postmortem CT images, and it is worth understanding these routine artifacts in order to distinguish them from abnormal findings (11). However, postmortem changes sometimes mimic pathologic lesions and vice versa. Although several studies have examined postmortem CT findings in individual organs (12-18), few have evaluated postmortem changes on whole-body postmortem CTs (19, 20). In this pictorial essay, we present a case series of atraumatic in-hospital deaths, characterize the postmortem imaging features on postmortem CT, and discuss the pitfalls of postmortem CT examination and the differential diagnosis of postmortem CT findings.

### Intracranial High Density in the Extra-Axial Brain Space

Hypostasis is the earliest postmortem change and occurs in all fluid compartments, tissues, and organs (21). Its distribution shifts as the body is repositioned, and the tissue blanches with external pressure (22, 23). After

circulation ceases, the concentrated red blood cells exhibit hypostasis under gravity (24, 25). On brain postmortem CT, hypostasis increases the density in the dorsal superior sagittal sinus (SSS) beyond its initial value from the antemortem CT (AMCT) (26). When interpreting a brain postmortem CT, we often observe high density in the extra-axial brain space, mimicking normal postmortem hypostasis in the SSS.

In case 1, high density was observed in the dorsal SSS and was initially considered a normal postmortem change (Fig. 1A, arrowhead). However, linear and curving high-density lesions were identified along the falx cerebri and cerebral sulcus (Fig. 1A, arrows); therefore, subarachnoid hemorrhage or subdural hematoma was suspected. An autopsy revealed diffuse subarachnoid hemorrhage (Fig. 1B). Potentially, high-density areas in the extra-axial brain space may be misinterpreted as normal postmortem changes when the high-density region is adjacent to an area of hypostasis. When the location of a high-density area matches that of the superficial cerebral veins, postmortem intravascular coagulation may be present.

## Gross Postmortem CT Images of the Brain

Brain swelling and a loss of distinction between the gray matter (GM) and white matter (WM) are normal postmortem changes on postmortem CT. Takahashi et al. (27) reported that postmortem brain autolysis may occur without concurrent vasogenic edema owing to hyperacute global ischemia in the absence of reperfusion; as a result, a subtle loss of distinction between the GM and WM can be detected on early postmortem CT. The ventricles and cisterns are sometimes visibly effaced because of mild swelling during the immediate postmortem period (27, 28). The GM and WM densities are considerably higher on postmortem CT than on AMCT, which reflects the presence of severe hypoxic-anoxic encephalopathy before death. The GM density is normally higher than the WM density on AMCT (29-32).

In cases 2, 3, and 4, three patterns were observed on brain postmortem CT. These cases indicate that the following patterns may be found in the brain following an in-hospital atraumatic death: 1) unremarkable postmortem change (Fig. 2A); 2) brain swelling represented by decreases in the ventricle and sulci sizes (Fig. 2B); and 3) diffuse brain swelling with absent GM-WM distinction (Fig. 2C). In cases 2, 3, and 4, death occurred 1 hour and 35 minutes, 9 hours and 9 minutes, and 14 hours and 41 minutes after the postmortem CT, respectively. These patterns may be interpreted differently depending on patient characteristics such as age or concurrent antemortem lesions. It remains unclear how these postmortem CT findings reflect the antemortem pathology or the interval between death and
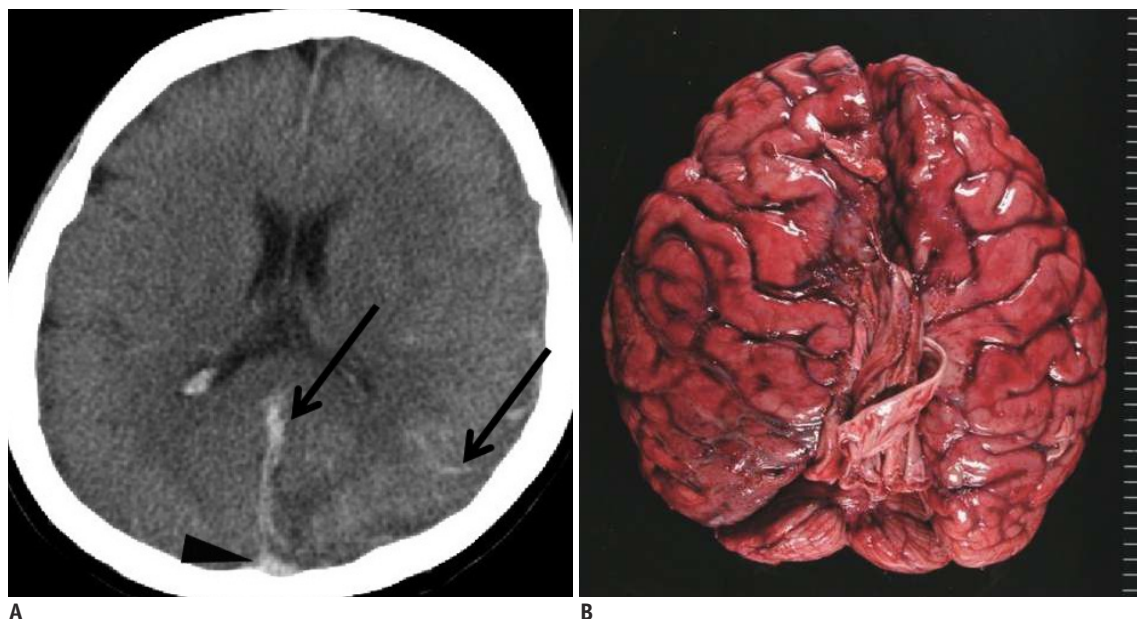


**Fig. 1. Hypostasis and hemorrhagic lesion in brain in 35-year-old deceased woman (case 1).**
**A.** CT scan obtained 8 hours and 35 minutes after death shows obscure hypostasis in dorsal superior sagittal sinus (arrowhead) in case 1. Linear and curving high density lesions are present along falx cerebri and cerebral sulcus (arrows). **B.** Subsequent autopsy reveals diffuse subarachnoid hemorrhage. CT = computed tomography

postmortem CT, and whether the postmortem elapsed time and magnitude of brain swelling are correlated (33).

## High Density in the Heart and Great Vessels

Hypostasis in the heart and great vessels often forms a fluid–fluid level, increasing the hematocrit to 80% in the dependent region of the cadaver. During hypostasis, the concentrated red blood cells exhibit intravascular sedimentation on postmortem CT, as the plasma and cellular components sink with gravity (24, 25).

In case 5, hypostasis was observed in the thoracic aorta on postmortem CT (Fig. 3A, arrow). In the left pulmonary artery, an immobile hyperdense cast was detected (Fig. 3A, arrowheads) and differed from the left atrium and thoracic aorta findings, which formed a fluid–fluid level, and also from postmortem clotting, which was mostly concentrated in a free-floating manner near the horizontal border of the hypostasis within the large vessels. Thus, pulmonary thrombosis was suspected and subsequently



**A**        **B**        **C**
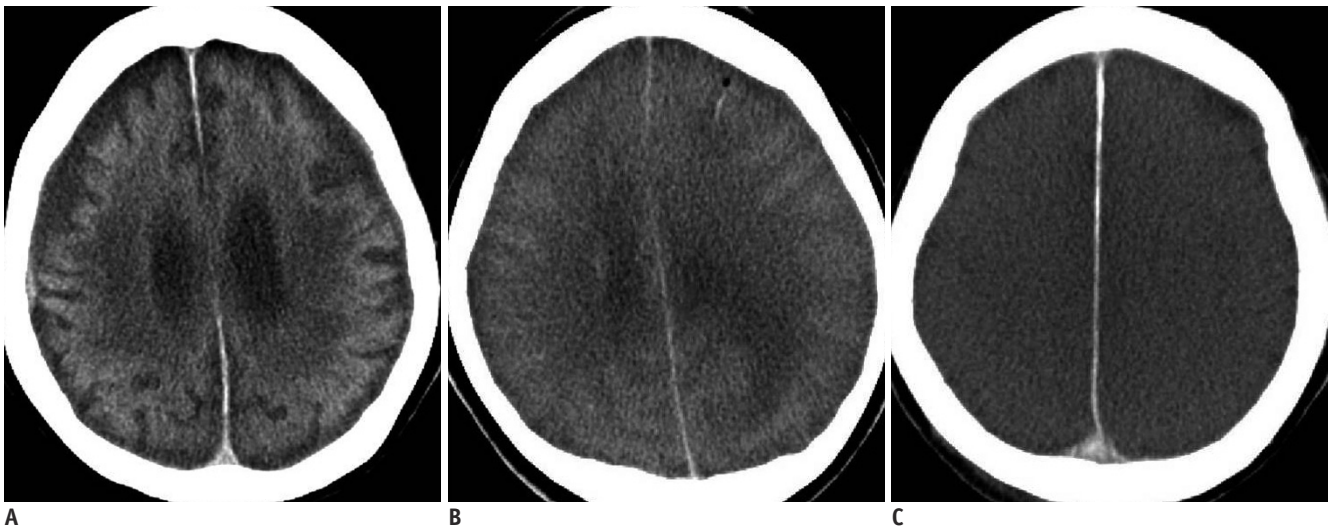
**Fig. 2. Three lesion patterns on postmortem CT images of brain.**
**A.** Pattern 1. CT scan of 53-year-old deceased woman obtained 1 hour and 35 minutes after death shows unremarkable postmortem changes (case 2). **B.** Pattern 2. CT scan of 39-year-old deceased woman obtained 9 hours and 9 minutes after death shows diffuse brain swelling (case 3). **C.** Pattern 3. CT scan of 78-year-old deceased man obtained 14 hours and 41 minutes after death shows both diffuse brain swelling and loss of distinction between gray and white matter (case 4). CT = computed tomography



**A**        **B**
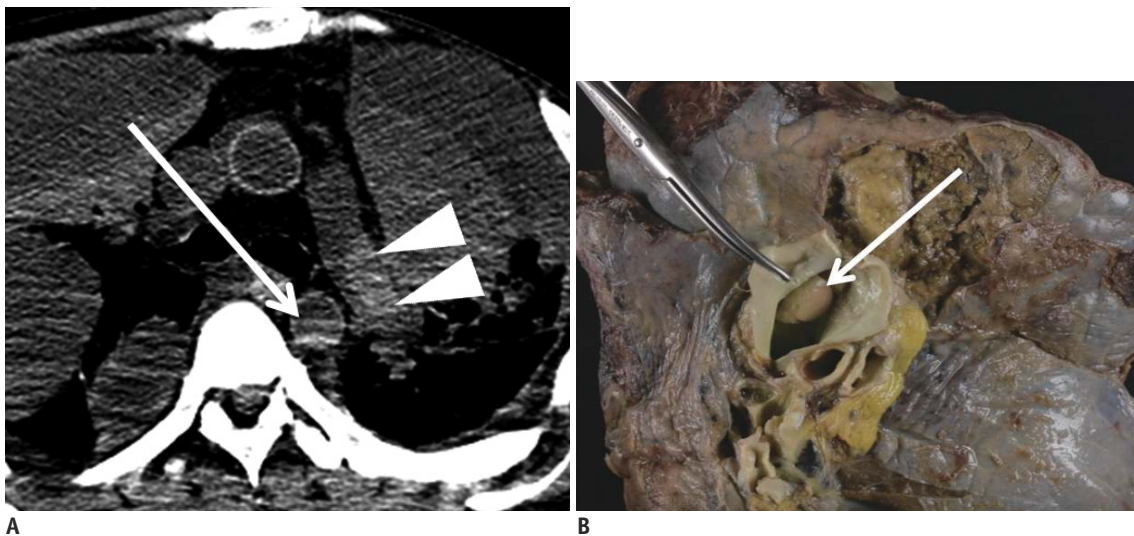
**Fig. 3. Hypostasis and thrombosis in great vessels in 45-year-old deceased man (case 5).**
CT scan obtained 2 hours and 8 minutes after death shows hypostasis in thoracic aorta (**A**, arrow). Hyperdense cast is present within left pulmonary artery (**A**, arrowheads), which is later diagnosed as pulmonary thrombus on autopsy (**B**, arrow). CT = computed tomography

confirmed on autopsy (Fig. 3B, arrow). Although pulmonary thrombosis varies in density and form, it is distinguishable from hypostasis. The key features suggesting pulmonary thrombus are a blood clot with a non-fluid–fluid level and hyperdense cast formation occluding the pulmonary artery (34-36). However, this standard should not be applied when the posture of the cadaver is changed.

Aortic dissection also mimics hypostasis on postmortem CT. In case 6, a flap separating two lumens and hypostasis were observed within the ascending aorta on postmortem CT (Fig. 4, arrow and arrowheads, respectively). Both lesions exhibited high density. Increased density and aortic wall thickening, which are normal postmortem changes, were also observed (Fig. 4, dotted arrow). Several studies have evaluated the postmortem changes in the aorta. Okuma et al. (18) observed an increased aortic wall thickness on postmortem CT compared with AMCT in the same patients, and Shiotani et al. (37) reported an increased aortic wall density on postmortem CT. This increased density may be confused with aortic dissection by radiologists who are inexperienced with postmortem imaging. Takahashi et al. (38) and Hyodoh et al. (39) similarly described the postmortem changes in the aortic form. They reported that the aortic diameter and overall size decreased postmortem. The descending thoracic and abdominal aorta in particular became ovoid (38). These deformations are considered
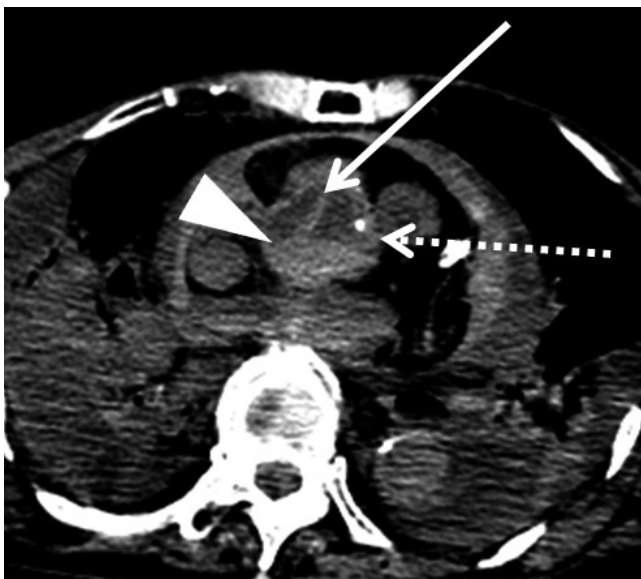


**Fig. 4. Dissection and hypostasis in ascending aorta in 76-year-old deceased woman (case 6).** CT scan obtained 14 hours and 30 minutes after death shows both flap (arrow) separating two lumens and hypostasis (arrowhead) in ascending aorta. Increased density and thickening of aortic wall, which are normal postmortem changes, are also observed (dotted arrow). CT = computed tomography

normal postmortem changes.

## Increased Lung Density and Fluid within Airways

Hypostasis occurs in numerous organs, and the lung is no exception. The density of lung parenchyma in the dependent region increases over time, and a gradient density is observed after a certain duration postmortem (5, 40).

In case 7, increased pulmonary density with a nearly horizontal border was observed in the dependent region of the bilateral upper lobes (Fig. 5A, arrows) and typifies postmortem lung hypostasis. This high pulmonary density on postmortem CT is characterized by a horizontal, gravity-dependent border and is often bilaterally symmetrical. In contrast, an asymmetrical and segmental increase in lung density on postmortem CT indicates a pathologic lesion and may be diagnosed in the same manner as on AMCT in daily practice. In this case, we suspected that the consolidation in right lower lobe was inflammation (Fig. 5B). Histopathologic examination and the autopsy confirmed these suspicions; pulmonary congestion (Fig. 5C) and inflammatory cellular infiltration (pneumonia) (Fig. 5D), corresponding to Figure 5A and B, respectively, were observed on microscopy. Endotracheal fluid was also observed (Fig. 5A, arrowhead). In our previous study, fluid within the airway was frequently observed on postmortem CT in subjects with pleural effusion or atelectasis/pulmonary consolidation, and the volume of airway fluid increased over time postmortem (17).

In case 8, multiple areas of consolidation and randomly distributed nodules were found on postmortem CT (Fig. 6). These findings were quite distinct from typical postmortem changes such as hypostasis, and the autopsy revealed pneumonia. Uncharacteristic or atypical postmortem changes on postmortem CT should be closely examined because these findings can indicate antemortem pathology such as inflammation, tumors, or other lesions.

## Intraorganic/Vascular Gas

Intraorganic/vascular gas is a common finding on postmortem CT, and two mechanisms have been proposed for gas development: cardiopulmonary resuscitation (CPR) (41-47) and decomposition (20, 43, 48-50). Decomposition gas reportedly occurs within 24–48 hours postmortem and is typically produced by intestinal flora (48). Antemortem
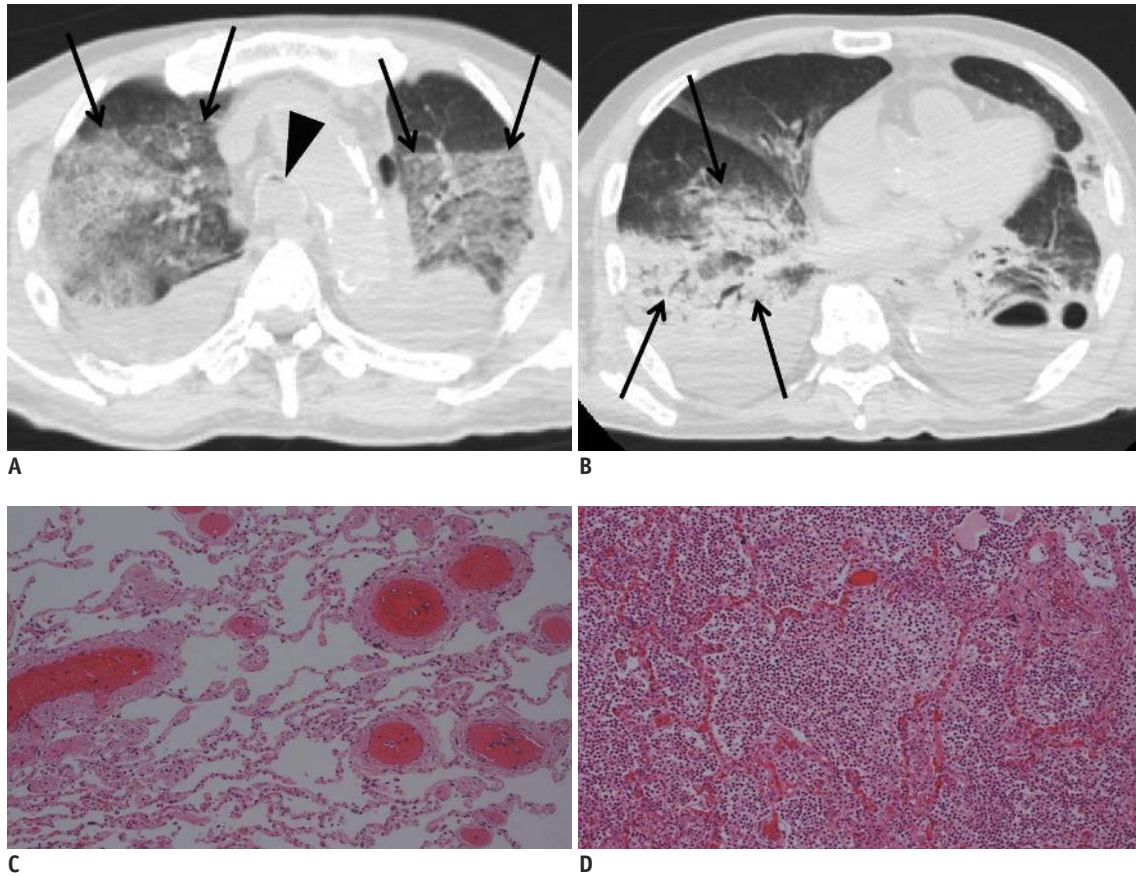
**Fig. 5. Hypostasis and pathologic lesion in lung in 73-year-old deceased man (case 7).**
**A.** CT scan obtained 16 hours and 48 minutes after death shows increased density lesion with horizontal border in dependent region of left upper lobe, which is attributed to hypostasis (arrows). Endotracheal fluid, thought to be normal postmortem change, is also observed (arrowhead). **B.** Asymmetrical and segmental consolidation is simultaneously observed in right lower lobe (arrows). **C, D.** Pathological examination with hematoxylin and eosin on subsequent autopsy indicates pulmonary congestion (C; low-power view) and inflammatory cellular infiltration (pneumonia) (D; low-power view). Images **C** and **D** correspond to **A** and **B**, respectively. CT = computed tomography

sepsis has been associated with rapid decomposition and putrefaction postmortem (51). The state of preservation (i.e., atmospheric temperature and humidity) also affects the generation of decomposition gas (42, 49). The exact mechanism allowing bacteria to survive in the human body and produce gas is unclear (49).

A different theory suggests that intravascular gas is produced during CPR. Chest compression causes the vaporization of dissolved gas in blood (42, 45), and the rupture of pulmonary vessels combined with lung parenchymal destruction permits air to enter the pulmonary vein and reach the systemic circulation (45-47). Furthermore, in a state of ischemia and tissue damage, bronchovenous fistulas, which are presumably caused by endotracheal intubation (42), may enable the production of intravenous gas. Positive-pressure ventilation causes barotrauma, potentially causing alveolar rupture (47, 52), and air enters the circulation during intravenous

catheterization (45).

In case 9, broad areas of intraorganic/vascular gas were detected (Fig. 7). CPR was not performed because the patient had a do-not-resuscitate (DNR) order. Although there was no evidence of clinical sepsis in this case, the potential for sepsis during the agonal stage or for postmortem decomposition gas should be considered in similar cases. Radiologists should also inform pathologists of the presence of intraorganic/vascular gas on postmortem CT in order to help in the subsequent diagnosis, as this gas can never be found by autopsy. Notably, intraorganic/vascular gas is not always observed on postmortem CT, even in patients that received CPR or those with sepsis (15).

## Fluid in the Gastrointestinal Tract

Gastrointestinal (GI) tract fluid is a nonspecific finding. The GI density varies with numerous factors such as blood,

certain medications (particularly laxatives), oral contrast medium, food, and others. GI content is often hyperdense on both AMCT and postmortem CT; therefore, diagnosing a
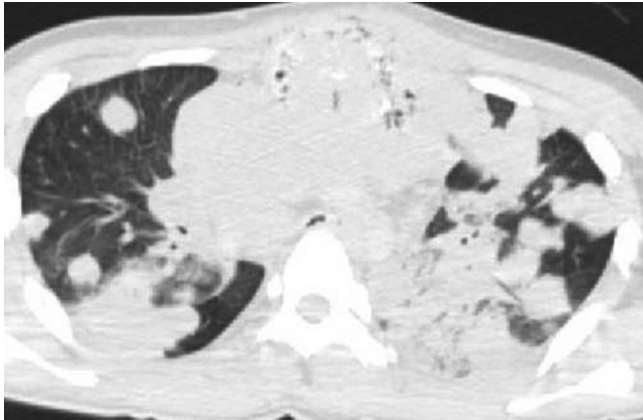


**Fig. 6. Hyperdense lung lesion not attributed to normal postmortem change in 18-year-old deceased man (case 8).**
CT scan obtained 3 hours and 32 minutes after death shows multiple areas of consolidation and randomly distributed nodules. Subsequent autopsy revealed pneumonia. CT = computed tomography

GI hemorrhage can be difficult.

In case 10, the patient had a history of liver cirrhosis, which was detected on postmortem CT, as were esophagogastric varices. On postmortem CT, the gastric contents showed two different densities. We suspected that the higher density material resulted from a rupture of the esophagogastric varices (Fig. 8), which was confirmed on the subsequent autopsy. The two differing densities within the gastric lumen on postmortem CT were identified as hemorrhage and food on autopsy. This case suggests that higher density material in the gastric lumen clumps and covers less dense material, and that the existence of liver cirrhosis and esophageal varices may be a cause of intragastric hematoma. The medical history before death can suggest the source of mixed density fluid identified on postmortem CT.

Two other types of hyperdense GI fluids were observed in cases 11 and 12. In case 11, the colon contained mildly hyperdense fluid on the postmortem CT (Fig. 9), which
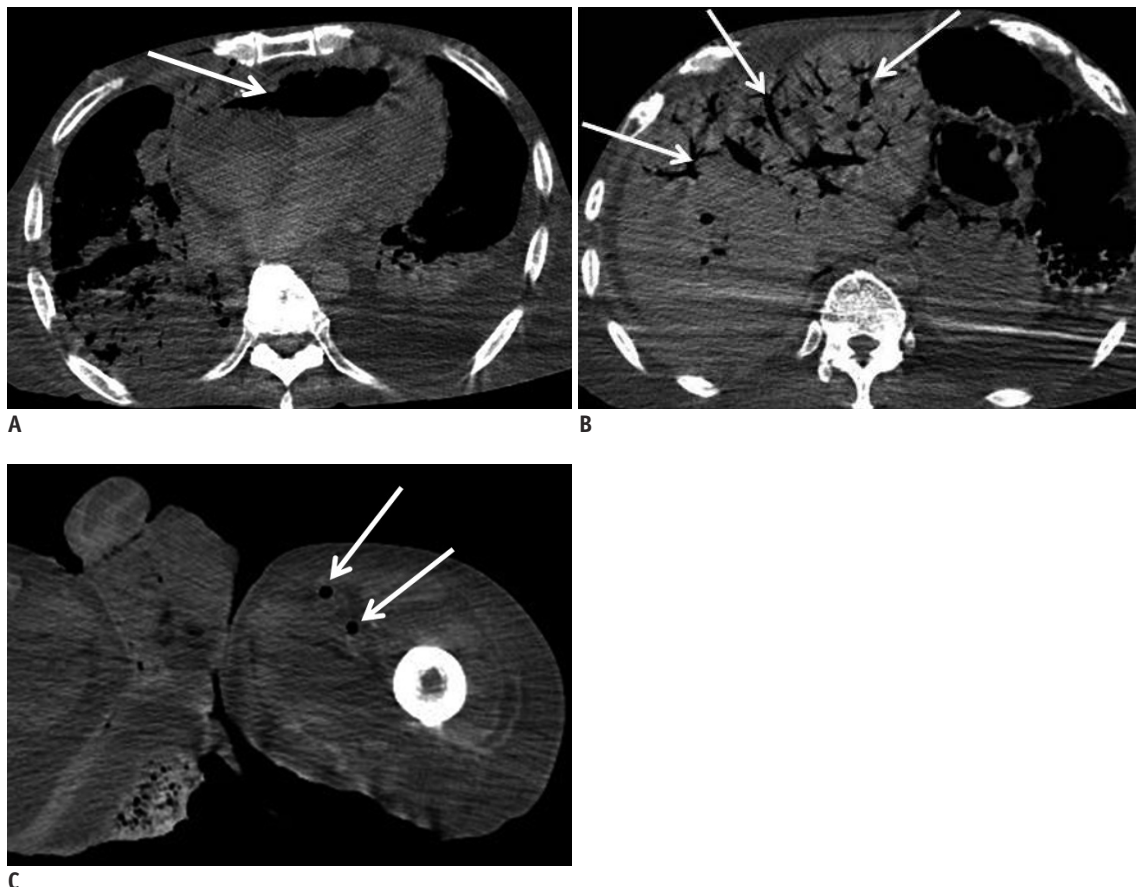


**Fig. 7. Broad intraorganic/vascular gas unassociated with cardiopulmonary resuscitation (CPR) in 65-year-old deceased man (case 9).**
CT scan obtained 12 hours and 20 minutes after death shows intraorganic/vascular gas throughout body (A-C, arrows). Gas is observed within lumens of right atrium and ventricle (A), and left femoral artery and vein (C). Intrahepatic gas is also observed (B), which is considered to be in hepatic vascular system. CPR was not performed because patient had do-not-resuscitate order. CT = computed tomography

was identified as a hemorrhage on autopsy. His medical records indicated that he was receiving anticoagulant medication and thus at risk of hemorrhage. In case 12, the colon contained extremely hyperdense contents (Fig. 10). The material was not hemorrhagic on autopsy, and its identity was unclear. It was also unclear whether the patient was administered a laxative or oral contrast medium antemortem. These cases highlight the difficulty in determining the source of hyperdense GI fluid using postmortem CT alone.

## Hyperdense Wall of the GI Tract

Compared to the GI lumen, intramural hemorrhage in the GI tract is difficult to diagnose, even on AMCT (53). When fluid within the GI tract is water-dense, the GI wall density is typically high on postmortem CT. However, a hyperdense GI wall on postmortem CT should be evaluated carefully because it can indicate intramural hemorrhage. For example, in case 13, hyperdense walls were widespread throughout the GI tract (Fig. 11A). This finding was identified as

intramural hemorrhage on the subsequent autopsy (Fig. 11B, C).

## Luminal Gas in the GI Tract

Gas dilatation of the GI tract can be caused by CPR. Bag-valve-mask ventilation sends air into both the trachea and esophagus. As a result, a massive volume of air is delivered to the GI tract, causing GI distension for some time after



**Fig. 9. Hemorrhagic hyperdense fluid in colon in 50-year-old deceased woman (case 11).** CT scan obtained 2 hours and 17 minutes after death shows hyperdense contents, which fill colon (arrows) and were diagnosed as hemorrhagic on autopsy. Upon reviewing patient's medical history, we found that he was receiving anticoagulant medication and thus was at risk of hemorrhage. CT = computed tomography



**Fig. 8. Hemorrhagic hyperdense fluid in stomach in 65-year-old deceased woman with liver cirrhosis and esophagogastric varices (case 10).** CT scan obtained 13 hours and 33 minutes after death shows content with two different densities in gastric lumen. Higher density material in gastric lumen (arrows) is clumped, covers lower density material, and is suspected to be caused by rupture of esophagogastric varices. This was proven on subsequent autopsy. CT = computed tomography



**Fig. 10. Non-hemorrhagic hyperdense fluid in colon in 72-year-old deceased woman (case 12).** CT scan obtained 1 hours and 48 minutes after death shows hyperdense content in colon (arrow) similar to case 11. However, this material was not hemorrhagic on subsequent autopsy. It was unclear based on patient's medical history whether she was administered oral contrast medium or other oral medication, such as laxative. Residual contrast material is also observed in kidneys of cases 12 and 16 because contrast-enhanced CT was performed immediately before death. CT = computed tomography
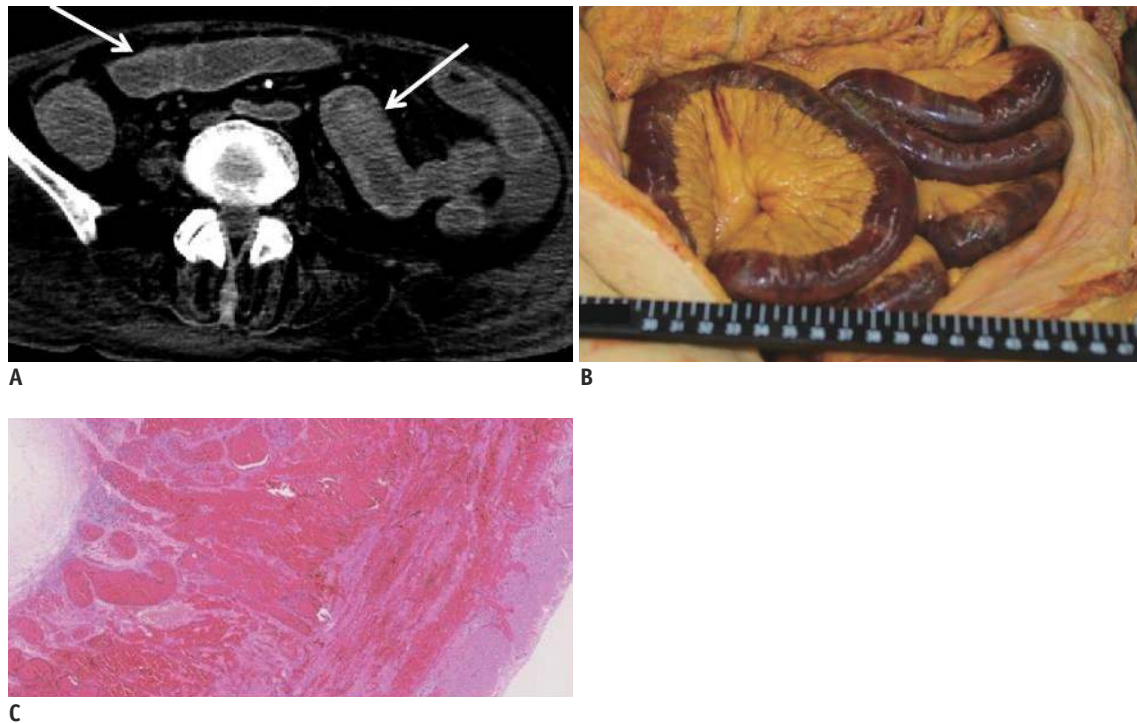
Fig. 11. Hyperdense wall of GI tract in 74-year-old deceased woman (case 13).
**A.** CT scan obtained 2 hours and 34 minutes after death shows hyperdense walls throughout GI tract (arrows). **B, C.** Autopsy revealed that hyperdense GI wall was intramural hemorrhage (**B**, macroscopic image; **C**, microscopic low-power view image with hematoxylin and eosin stain). CT = computed tomography, GI = gastrointestinal

artificial respiration is discontinued (43).

In case 14, CPR was not performed because of the patient's DNR order. Although GI distension was observed on postmortem CT (Fig. 12), this finding is not always associated with CPR and may occasionally be observed in patients who do not receive CPR. The source of the massive gas volume in this case was unclear, and the finding is nonspecific. However, postmortem CT images with this abnormality require careful interpretation because GI dilatation on postmortem CT in a patient who does not receive CPR may indicate a bowel obstruction caused by a tumor, feces, volvulus, or other condition.

Intrahepatic gas has a well-known association with GI distension on postmortem CT. Shiotani et al. (43) reported that the grade of hepatic portal venous gas increased significantly as the severity of GI distension increased on postmortem CT. Thus, it is important to assess the relationship between GI distension and intraorganic/vascular gas when these findings are found on postmortem CT images.

## Intramural Gas in the GI Tract

Intramural gas in the GI tract on postmortem CT is
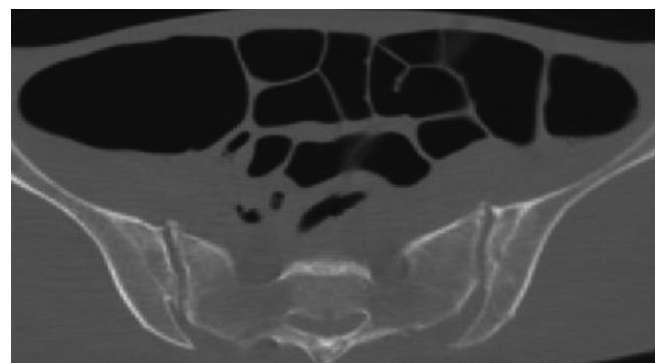


Fig. 12. Intraluminal gas in GI tract unassociated with CPR in 64-year-old deceased man (case 14). CT scan obtained 3 hours and 57 minutes after death shows widespread distension of GI tract. Although this finding can be caused by CPR, in this patient, CPR was not performed due to DNR order. This finding is considered nonspecific. CPR = cardiopulmonary resuscitation, CT = computed tomography, DNR = do-not-resuscitate, GI = gastrointestinal

considered a normal postmortem change caused by mucosal injury after circulation ceases. Immediately before death, the GI tract is in a state of extreme ischemia, which induces severe mucosal damage that enhances mucosal permeability and permits the passage of intraluminal gas into the GI wall. Particularly, in patients who receive CPR through bag-valve-mask ventilation, intramural or hepatic portal venous gas is reportedly accompanied by GI distension (54, 55).

In one CPR case (case 15), broad areas of intramural gas were observed throughout the GI tract on postmortem CT (Fig. 13). Although CPR may have contributed, the autopsy proved that he had pneumatosis cystoides intestinalis. Thus, the cause of intramural gas in the GI tract may not be due solely to CPR and occasionally reflects an antemortem condition.

In one patient who did not receive CPR (case 16), intramural gas was observed in the ascending colon on postmortem CT (Fig. 14). The microscopic examination and autopsy did not reveal any significant pathology associated with the intramural gas found on postmortem CT. Therefore, the gas was attributed to mucosal injury secondary to non-pathological postmortem change. As indicated by this particular case, the relationship between intramural gas in the GI tract on postmortem CT and antemortem CPR is not readily evident.

## Dilatation of the Right Heart

Right-heart dilatation is often observed on postmortem CT and is a well-described and normal postmortem change caused by blood congestion (56, 57). Therefore, it is difficult to diagnose right heart failure as the cause of death using postmortem CT.

In case 17, we diagnosed pulmonary veno-occlusive disease on autopsy, which is a rare disease and was not suspected on postmortem CT. On postmortem CT, the right

heart dilatation was more prominent than usual for a normal postmortem change (Fig. 15A), and pulmonary artery dilation (Fig. 15B) and pulmonary edema were present (Fig. 15C). In hindsight, if these findings were comprehensively evaluated, then pulmonary veno-occlusive disease may have been diagnosed on postmortem CT.

## Summary

Postmortem CT images are more easily interpreted when we consider that the findings are subject to three factors: the cause of death and associated pathology, normal postmortem changes, and the effect of CPR. Importantly, postmortem CT images should be interpreted
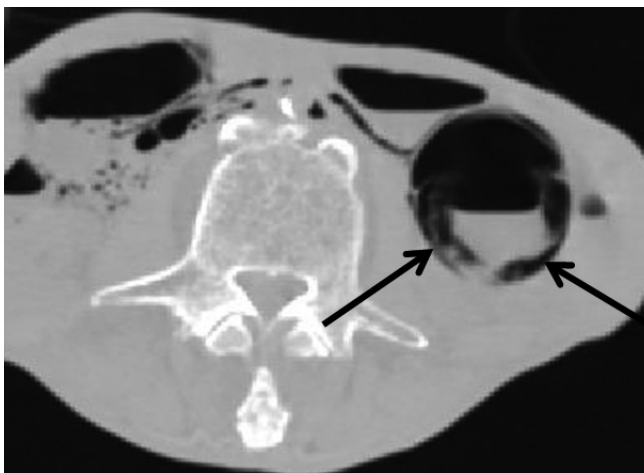


**Fig. 13. Intramural gas in GI tract caused by antemortem condition in 75-year-old deceased man who underwent CPR (case 15).** CT scan obtained 4 hours and 21 minutes after death shows intramural gas throughout GI tract (arrows). Although there may have some contribution from CPR, autopsy proved that he had pneumatosis cystoides intestinalis. CT = computed tomography, GI = gastrointestinal



**Fig. 14. Intramural gas in GI tract unassociated with CPR in 72-year-old deceased woman who did not undergo CPR (case 16).** CT scan obtained 1 hour and 48 minutes after death shows intramural gas throughout GI tract (arrows) similar to case 15. CPR was not performed before death due to patient's DNR order. However, autopsy did not reveal any pathology associated with this postmortem CT finding. Therefore, intramural gas was attributed to mucosal injury, which is normal postmortem change. CPR = cardiopulmonary resuscitation, CT = computed tomography, DNR = do-not-resuscitate, GI = gastrointestinal
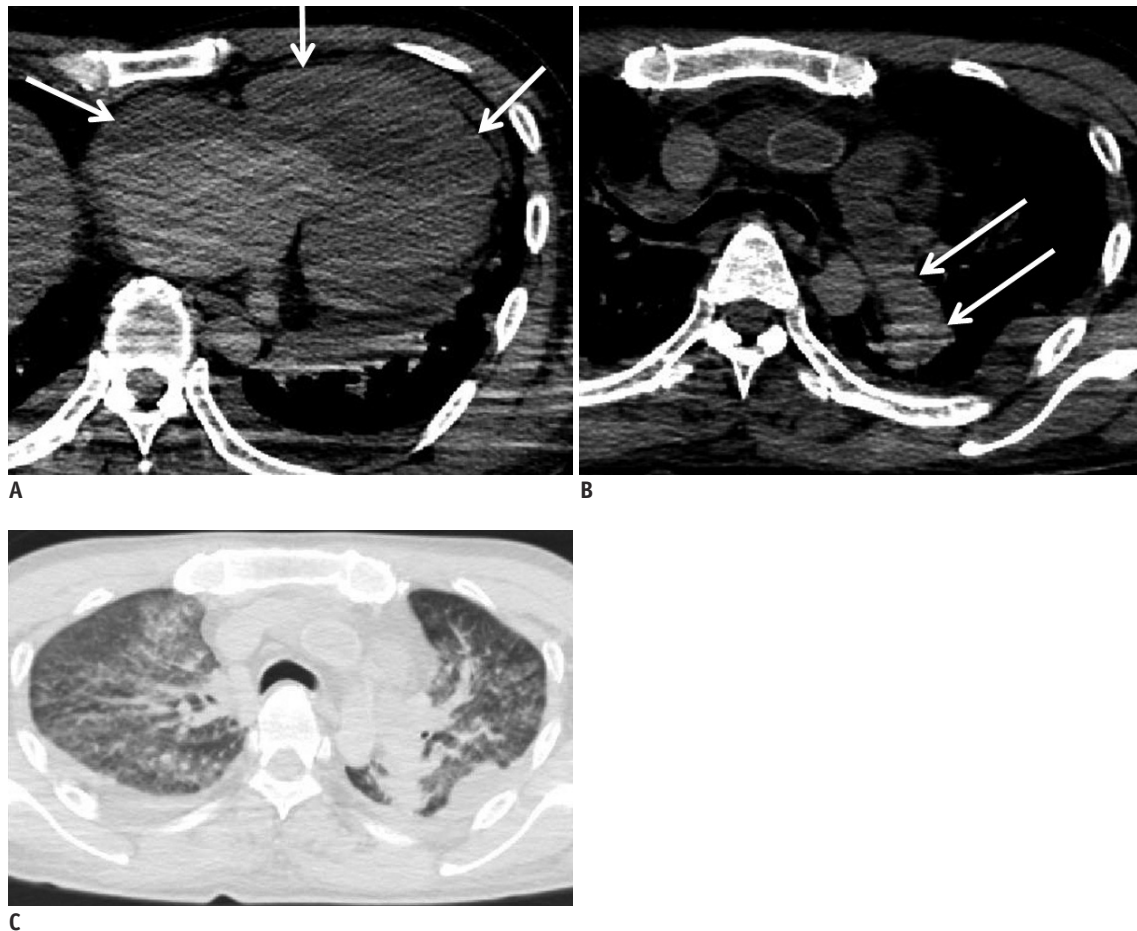
**Fig. 15. Dilatation of right heart in 50-year-old deceased man (case 17).**
CT scan obtained 17 hours and 18 minutes after death shows dilatation of right heart (**A**, arrows). Although this is known to be normal postmortem change caused by blood congestion, it became clear with in autopsy that finding in this case was caused by pulmonary veno-occlusive disease. Other lesions related to this disease are also present: pulmonary artery dilation (**B**, arrows) and pulmonary edema **(C)**. CT = computed tomography

comprehensively while considering the entire case, including the medical history, antemortem clinical course (medications and treatments), clinical data (laboratory data, microbiological culture, etc.), and other factors. Radiologists must carefully interpret postmortem CT images as findings that initially appear to be normal postmortem changes may actually be pathologic. It is important that clinicians not take for granted that common findings on postmortem CT are often normal postmortem changes. Conversely, radiologists must be careful to avoid misinterpreting a normal postmortem change as an antemortem lesion.

## REFERENCES

1. Patriquin L, Kassarjian A, Barish M, Casserley L, O'Brien M, Andry C, et al. Postmortem whole-body magnetic resonance imaging as an adjunct to autopsy: preliminary clinical experience. *J Magn Reson Imaging* 2001;13:277-287

2. Thali MJ, Yen K, Schweitzer W, Vock P, Boesch C, Ozdoba C, et al. Virtopsy, a new imaging horizon in forensic pathology: virtual autopsy by postmortem multislice computed tomography (MSCT) and magnetic resonance imaging (MRI)--a feasibility study. *J Forensic Sci* 2003;48:386-403

3. Ezawa H, Yoneyama R, Kandatsu S, Yoshikawa K, Tsujii H, Harigaya K. Introduction of autopsy imaging redefines the concept of autopsy: 37 cases of clinical experience. *Pathol Int* 2003;53:865-873

4. Roberts IS, Benamore RE, Benbow EW, Lee SH, Harris JN, Jackson A, et al. Post-mortem imaging as an alternative to autopsy in the diagnosis of adult deaths: a validation study. *Lancet* 2012;379:136-142

5. Shiotani S, Kohno M, Ohashi N, Yamazaki K, Nakayama H, Watanabe K, et al. Non-traumatic postmortem computed tomographic (PMCT) findings of the lung. *Forensic Sci Int* 2004;139:39-48

6. Aghayev E, Sonnenschein M, Jackowski C, Thali M, Buck U, Yen K, et al. Postmortem radiology of fatal hemorrhage:

measurements of cross-sectional areas of major blood vessels and volumes of aorta and spleen on MDCT and volumes of heart chambers on MRI. *AJR Am J Roentgenol* 2006;187:209-215

7. Jackowski C, Schweitzer W, Thali M, Yen K, Aghayev E, Sonnenschein M, et al. Virtopsy: postmortem imaging of the human heart in situ using MSCT and MRI. *Forensic Sci Int* 2005;149:11-23

8. Kobayashi T, Shiotani S, Kaga K, Saito H, Saotome K, Miyamoto K, et al. Characteristic signal intensity changes on postmortem magnetic resonance imaging of the brain. *Jpn J Radiol* 2010;28:8-14

9. Ishida M, Gonoi W, Hagiwara K, Takazawa Y, Akahane M, Fukayama M, et al. Postmortem changes of the thyroid on computed tomography. *Leg Med (Tokyo)* 2011;13:318-322

10. Ishida M, Gonoi W, Hagiwara K, Okuma H, Shirota G, Shintani Y, et al. Early postmortem volume reduction of adrenal gland: initial longitudinal computed tomographic study. *Radiol Med* 2015;120:662-669

11. Shiotani S, Takahashi N, Anzai Y, Hasegawa I, Yamamoto S, Oguma E, et al. *Guidelines for interpretation of postmortem CT*. In: Imai Y, Takano H, Yamamoto S, eds. *Autopsy imaging guideline*, 2nd ed. Tokyo: Vector Core, 2012:54-68

12. Okuma H, Gonoi W, Ishida M, Shintani Y, Takazawa Y, Fukayama M, et al. Heart wall is thicker on postmortem computed tomography than on antemortem [corrected] computed tomography: the first longitudinal study. *PLoS One* 2013;8:e76026

13. Okuma H, Gonoi W, Ishida M, Shirota G, Shintani Y, Abe H, et al. Comparison of attenuation of striated muscle between postmortem and antemortem computed tomography: results of a longitudinal study. *PLoS One* 2014;9:e111457

14. Jackowski C, Thali MJ, Buck U, Aghayev E, Sonnenschein M, Yen K, et al. Noninvasive estimation of organ weights by postmortem magnetic resonance imaging and multislice computed tomography. *Invest Radiol* 2006;41:572-578

15. Ishida M, Gonoi W, Hagiwara K, Takazawa Y, Akahane M, Fukayama M, et al. Intravascular gas distribution in the upper abdomen of non-traumatic in-hospital death cases on postmortem computed tomography. *Leg Med (Tokyo)* 2011;13:174-179

16. Ishida M, Gonoi W, Hagiwara K, Takazawa Y, Akahane M, Fukayama M, et al. Hypostasis in the heart and great vessels of non-traumatic in-hospital death cases on postmortem computed tomography: relationship to antemortem blood tests. *Leg Med (Tokyo)* 2011;13:280-285

17. Ishida M, Gonoi W, Hagiwara K, Okuma H, Shintani Y, Abe H, et al. Fluid in the airway of nontraumatic death on postmortem computed tomography: relationship with pleural effusion and postmortem elapsed time. *Am J Forensic Med Pathol* 2014;35:113-117

18. Okuma H, Gonoi W, Ishida M, Shintani Y, Takazawa Y, Fukayama M, et al. Greater thickness of the aortic wall on postmortem computed tomography compared with antemortem computed tomography: the first longitudinal

study. *Int J Legal Med* 2014;128:987-993

19. Cha JG, Kim DH, Kim DH, Paik SH, Park JS, Park SJ, et al. Utility of postmortem autopsy via whole-body imaging: initial observations comparing MDCT and 3.0 T MRI findings with autopsy findings. *Korean J Radiol* 2010;11:395-406

20. Levy AD, Harcke HT, Mallak CT. Postmortem imaging: MDCT features of postmortem change and decomposition. *Am J Forensic Med Pathol* 2010;31:12-17

21. Shepherd R. *Simpson's forensic medicine*, 12th ed. London: Arnold, 2003:37-41

22. Di Maio VJ, Di Maio DJ. *Forensic pathology*, 2nd ed. Boca Raton: CRC Press, 2001:21-26

23. Payne-James J, Busuttil A, Smock W. *Forensic medicine: clinical and pathological aspects*, 1st ed. San Francisco: Greenwich Medical Media, 2002:731-746

24. Shiotani S, Kohno M, Ohashi N, Yamazaki K, Itai Y. Postmortem intravascular high-density fluid level (hypostasis): CT findings. *J Comput Assist Tomogr* 2002;26:892-893

25. Jackowski C, Thali M, Aghayev E, Yen K, Sonnenschein M, Zwygart K, et al. Postmortem imaging of blood and its characteristics using MSCT and MRI. *Int J Legal Med* 2006;120:233-240

26. Takahashi N, Satou C, Higuchi T, Shiotani M, Maeda H, Hirose Y. Quantitative analysis of intracranial hypostasis: comparison of early postmortem and antemortem CT findings. *AJR Am J Roentgenol* 2010;195:W388-W393

27. Takahashi N, Satou C, Higuchi T, Shiotani M, Maeda H, Hirose Y. Quantitative analysis of brain edema and swelling on early postmortem computed tomography: comparison with antemortem computed tomography. *Jpn J Radiol* 2010;28:349-354

28. Smith AB, Lattin GE Jr, Berran P, Harcke HT. Common and expected postmortem CT observations involving the brain: mimics of antemortem pathology. *AJNR Am J Neuroradiol* 2012;33:1387-1391

29. Dedouit F, Sévely A, Costagliola R, Otal P, Loubes-Lacroix F, Manelfe C, et al. Reversal sign on ante- and postmortem brain imaging in a newborn: report of one case. *Forensic Sci Int* 2008;182:e11-e14

30. Kjos BO, Brant-Zawadzki M, Young RG. Early CT findings of global central nervous system hypoperfusion. *AJR Am J Roentgenol* 1983;141:1227-1232

31. Bird CR, Drayer BP, Gilles FH. Pathophysiology of "reverse" edema in global cerebral ischemia. *AJNR Am J Neuroradiol* 1989;10:95-98

32. Han BK, Towbin RB, De Courten-Myers G, McLaurin RL, Ball WS Jr. Reversal sign on CT: effect of anoxic/ischemic cerebral injury in children. *AJNR Am J Neuroradiol* 1989;10:1191-1198

33. Sieswerda-Hoogendoorn T, Beenen LF, van Rijn RR. Normal cranial postmortem CT findings in children. *Forensic Sci Int* 2015;246:43-49

34. Jackowski C, Grabherr S, Schwendener N. Pulmonary thrombembolism as cause of death on unenhanced postmortem 3T MRI. *Eur Radiol* 2013;23:1266-1270

35. Tatco VR, Piedad HH. The validity of hyperdense lumen sign

in non-contrast chest CT scans in the detection of pulmonary thromboembolism. *Int J Cardiovasc Imaging* 2011;27:433-440

36. Cobelli R, Zompatori M, De Luca G, Chiari G, Bresciani P, Marcato C. Clinical usefulness of computed tomography study without contrast injection in the evaluation of acute pulmonary embolism. *J Comput Assist Tomogr* 2005;29:6-12

37. Shiotani S, Kohno M, Ohashi N, Yamazaki K, Nakayama H, Ito Y, et al. Hyperattenuating aortic wall on postmortem computed tomography (PMCT). *Radiat Med* 2002;20:201-206

38. Takahashi N, Higuchi T, Hirose Y, Yamanouchi H, Takatsuka H, Funayama K. Changes in aortic shape and diameters after death: comparison of early postmortem computed tomography with antemortem computed tomography. *Forensic Sci Int* 2013;225:27-31

39. Hyodoh H, Sato T, Onodera M, Washio H, Hasegawa T, Hatakenaka M. Vascular measurement changes observed using postmortem computed tomography. *Jpn J Radiol* 2012;30:840-845

40. Shiotani S, Kobayashi T, Hayakawa H, Kikuchi K, Kohno M. Postmortem pulmonary edema: a comparison between immediate and delayed postmortem computed tomography. *Leg Med (Tokyo)* 2011;13:151-155

41. Takahashi N, Higuchi T, Shiotani M, Maeda H, Hirose Y. Intrahepatic gas at postmortem multislice computed tomography in cases of nontraumatic death. *Jpn J Radiol* 2009;27:264-268

42. Jackowski C, Sonnenschein M, Thali MJ, Aghayev E, Yen K, Dirnhofer R, et al. Intrahepatic gas at postmortem computed tomography: forensic experience as a potential guide for in vivo trauma imaging. *J Trauma* 2007;62:979-988

43. Shiotani S, Kohno M, Ohashi N, Yamazaki K, Nakayama H, Watanabe K. Postmortem computed tomographic (PMCT) demonstration of the relation between gastrointestinal (GI) distension and hepatic portal venous gas (HPVG). *Radiat Med* 2004;22:25-29

44. Asamura H, Ito M, Takayanagi K, Kobayashi K, Ota M, Fukushima H. Hepatic portal venous gas on postmortem CT scan. *Leg Med (Tokyo)* 2005;7:326-330

45. Shiotani S, Kohno M, Ohashi N, Atake S, Yamazaki K, Nakayama H. Cardiovascular gas on non-traumatic postmortem computed tomography (PMCT): the influence of cardiopulmonary resuscitation. *Radiat Med* 2005;23:225-229

46. Yamaki T, Ando S, Ohta K, Kubota T, Kawasaki K, Hirama M. CT demonstration of massive cerebral air embolism from pulmonary barotrauma due to cardiopulmonary resuscitation. *J Comput Assist Tomogr* 1989;13:313-315

47. Hwang SL, Lieu AS, Lin CL, Liu GC, Howng SL, Kuo TH. Massive cerebral air embolism after cardiopulmonary resuscitation. *J Clin Neurosci* 2005;12:468-469

48. Sakata M, Miki A, Kazama H, Morita M, Yasoshima S. Studies on the composition of gases in the post-mortem body: animal experiments and two autopsy cases. *Forensic Sci Int* 1980;15:19-29

49. Singh MK, O'Donnell C, Woodford NW. Progressive gas formation in a deceased person during mortuary storage demonstrated on computed tomography. *Forensic Sci Med Pathol* 2009;5:236-242

50. Gill JR, Landi K. Putrefactive rigor: apparent rigor mortis due to gas distension. *Am J Forensic Med Pathol* 2011;32:242-244

51. Spitz WU, Spitz DJ, Fisher RS. *Spitz and Fisher's Medicolegal Investigation of Death: Guidelines for the Application of Pathology to Crime Investigation*, 4th ed. Springfield: Charles C Thomas, 2006:108

52. Shiotani S, Ueno Y, Atake S, Kohno M, Suzuki M, Kikuchi K, et al. Nontraumatic postmortem computed tomographic demonstration of cerebral gas embolism following cardiopulmonary resuscitation. *Jpn J Radiol* 2010;28:1-7

53. Chou CK, Mak CW, Tzeng WS, Chang JM. CT of small bowel ischemia. *Abdom Imaging* 2004;29:18-22

54. Benson MD. Adult survival with intrahepatic portal venous gas secondary to acute gastric dilatation, with a review of portal venous gas. *Clin Radiol* 1985;36:441-443

55. Edlich RF, Borner JW, Kuphal J. Gastric blood flow: its destruction during gastric distention. *Am J Surg* 1976;120:635-640

56. Christe A, Flach P, Ross S, Spendlove D, Bolliger S, Vock P, et al. Clinical radiology and postmortem imaging (Virtopsy) are not the same: specific and unspecific postmortem signs. *Leg Med (Tokyo)* 2010;12:215-222

57. Shiotani S, Kohno M, Ohashi N, Yamazaki K, Nakayama H, Watanabe K, et al. Dilatation of the heart on postmortem computed tomography (PMCT): comparison with live CT. *Radiat Med* 2003;21:29-35